4. An Investigation into the Propulsive Performance of a High Speed Container Ship with Triple Screws

Koichi YOKOO*, *Member*, Atsuo YAZAKI**, *Member*, Tatsuo ITO*, *Member*, Yasushi SUGIMURA***, *Member*, Hiroyuki KADOI*, *Member*, Mitsuhiro ABE***, *Member*, Nobuharu YOSHINO**, *Member*, Yoshihisa TSUKINO**, *Member*, Kazuo YAMAZAKI***, *Member*

(*From J.S.N.A. Japan Vol. 133, June 1973*)

Summary

Recent extension of the container transport system has lead to the remarkable increase in both speed and size of container ships. Since there is a practical limitation to the maximum out-put of an individual engine, multiple-screw propulsion will become necessary for a large container ship to attain a higher speed with a large capacity of transport than the speed of 25 knots. Comprehensive research works have been conducted with the aim at developing a high speed container ship with triple-screw to be built at Mitsui Shipbuilding & Engineering Co., Ltd. in 1972, for the service between Europe and Japan.

This report deals with comparative tests among single, twin and triple-screw propulsions, and with mutual interference between the hull and propellers, cavitation researches and full-scale measurements on the triple-screw ship. Such other items of research works as vibratory forces of the propellers will be reported in a later paper.

Principal conclusions obtained are as follows,

1) A triple-screw ship has a better propulsive performance than a twin-screw ship.

2) For the triple-screw ship adopted, inward rotation of the wing propellers gives better propulsive efficiency than outward rotation, which is explained both by the wake measurements by 5-hole pitot tubes and by the results of the self-propulsion tests.

3) Mutual interference between the center and wing propellers can be neglected practically.

4) The effect of variation of the propeller load on the self-propulsion factors of each propeller will be negligible, unless the variation is too large.

5) Added resistance of the appendages is also subject to the scale effect.

6) Decreasing the camber of the propeller section near the leading edge was shown to be an effective means to decrease the amount of back cavitation, both on the ship and on the model.

1. Introduction

Recent extension of the container transport system has lead to the remarkable increase in both speed and size of container ships, which requires high powered propulsion (Fig. 1)[1]. However, since there is a practical limitation to the maximum out-put of an individual engine, multiple-screw propulsion system will become necessary for a large container ship to attain a higher speed than about 25 knots. It may be usual thought that no. of shafts is increased from one to

* Ship Research Institute
** Shipbuilding Research Center of Japan
*** Mitsui Shipbuilding & Engineering Co., Ltd.

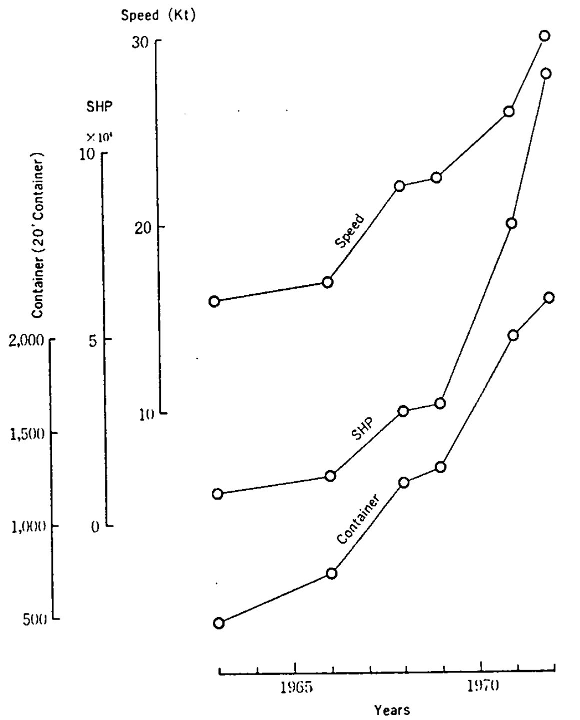

Fig. 1 Recent Trend of Speed, Horse Power etc. of Container Ships

two and from two to three with the increases of required out-put of the engine. No. of shafts should be properly chosen according to the ship's size and engine out-put, considering the propulsive performance, cavitation and vibratory forces of the propellers.

In a practical speed range of ordinary cargo ships a single screw ship is most superior in the propulsive performance, and the superiority of a single screw ship will be kept unchanged even if the ship became larger or even if the ship speed became higher. In a practical case, however, limitation to the propeller diameter will cause to decrease the propeller efficiency remarkably, which may not always maintain the superiority of a single screw.

If the propulsive performance were compared between twin and triple screws assuming that they have the same out-put of the engine, it will be clear that twin screws give not only lower propeller efficiency but also larger appendage resistance due to the larger bossing to support the screws. Moreover, twin screws will be inferior in the propulsive efficiency because they work in the region of the smaller wake. A triple screw ship seems to be superior to a twin screw ship according to the above consideration, and there is data[2] supporting this consideration.

Consequently, triple screw propulsion was adopted for a high speed container ship to serve between Europe and Japan, which was built in 1972 at Mitsui Shipbuilding and Engineering Co., Ltd.

This paper deals with the researches to develop this triple screw ship. To begin with, comparative tests were carried out among single, twin and triple screw ships. Then, on the triple screw ship, mutual interference among the hull and propellers was studied, and wake measurement, special self-propulsion test and cavitation test were performed. At last, various kinds of speed trials and cavitation observation were carried out on the full scale ship.

2. Comparison in Propulsive Performance among Single, Twin and Triple Screw Ships

2.1 *Model ships employed*

As be shown in Table 1, principal particulars and engine out-put are the same for single, twin and triple screw ships. These three ships have the same forebody shape deduced from the ample experience[3] in the hull forms of single screw ships. The afterbody shapes were so designed that the propeller, shaft and rudder arrangements may be suitable for each ship. The triple screw ship model is just the model of the actual triple screw ship to be built. The twin screw ship was designed to have the same form coefficient and similar bossings as those of the triple screw ship. The single screw ship was obtained by enlarging the principal particulars of a single screw ship already in service to have the same particulars as those of the triple screw ship. Stern arrangements of single, twin and triple screw ships are illustrated in Fig. 2. The propeller of each ship was designed to have the optimum efficiency at the rated no. of re-

Table 1 Particulars of Single-, Twin- and Triple-Screw Ships

		Single	Twin	Triple	
	L_{PP} (m)	252.000			
	B (m)	32.200			
	d (m)	11.000			
	C_B	0.575			
Main Engine	Position	Center	Wing	Center	Wing
	Kind	Turbine	Diesel	Diesel	Diesel
	No. of engine	1	2	1	2
	Out-put (PS)	80,000	40,000	32,000	24,000
	RPM	135	119	119	119
Propeller	Position	Center	Wing	Center	Wing
	No. of propeller	1	2	1	2
	No. of blades	6	6	6	6
	Dia. (m)	7.40	6.70	6.30	5.90
	H/D	1.29	1.22	1.29	1.29

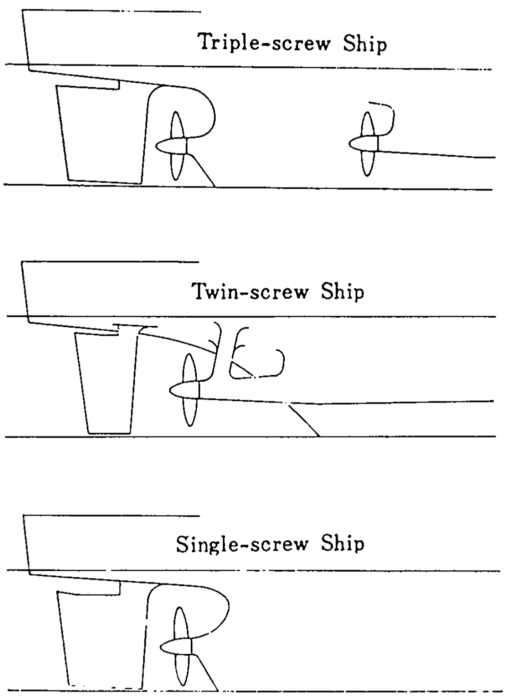

Fig. 2 Stern Arrangements of Single-, Twin- and Triple-Screw Ships

volutions of the assumed engine, using the design chart[4] of AU 6-85. Inward rotation was adopted for the propellers of the twin screw ship and the wing propellers of the triple screw ship, since it was already known that inward rotation gave better propulsive performance than outward rotation for this kind of hull form and bossing arrangement, the reason of which will be explained in the next chapter. It must be noted that no. of revolutions at the rated out-put for the single screw ship is much higher than that of the other ships.

2.2 *Model tests*

The model tests of the single and triple screw ships were carried out at the Shipbuilding Research Center of Japan and those of the twin screw ship at the Ship Research Institute. All the ship models were made of wood and 8 m in length. Fig. 3 shows the comparison of the results in resistance and propulsion tests on three ship models in the speed range between economical and maximum out-put. Residuary resistance coefficient r_R is the lowest on the single screw ship and highest on the twin screw ship. $(1-t)$ of the single screw ship is considerably larger than that of ordinary single screw ships. The reason for it will be in that the propeller diameter is relatively smaller because the assumed full scale ship is too large for a single screw ship. $(1-w)$ of the center propeller of the triple screw ship is quite larger than that of the single screw ship,

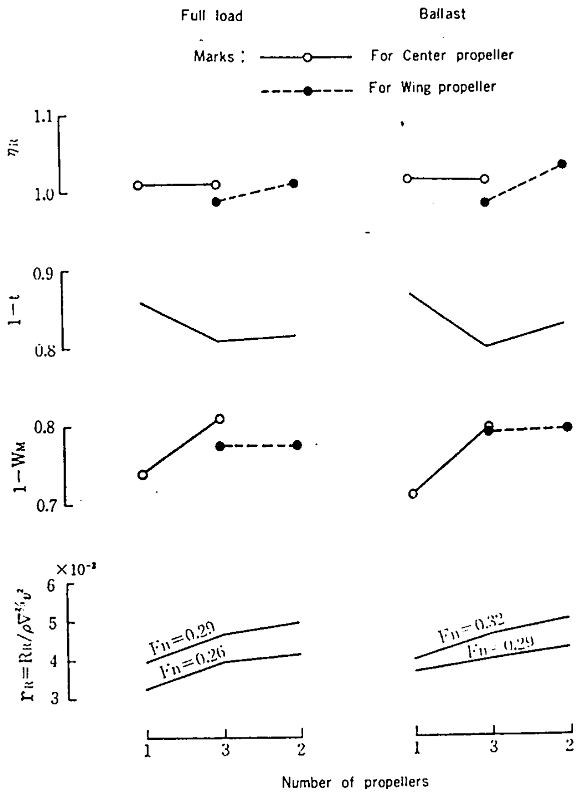

Fig. 3 Results of Resistance and Propulsion Tests for Single-, Twin- and Triple-Screw Ships

and $(1-w)$ of the wing propellers is nearly same as that of the twin screw ship. One reason, why $(1-w)$ of the wing propellers is smaller than that of the center propeller, will be attributed to the adoption of the inward rotation for the wing propellers, although the stern shape, propeller diameter and position will have some effects on this result.

In order to investigate the effect upon the resitance of the bossings, added resistance coefficient ΔC_A was obtained from the results of the resistance tests with and without bossings.

$$\Delta C_A=(R_{MA}-R_{MN})\Big/\frac{1}{2}\rho_M \Delta S_A v_M{}^2 \qquad (1)$$

Where,

R_{MA} and R_{MN}=total resistance with and without bossings

$\Delta S_A=(S_A-S_N)+$wetted surface area of the portion where the bossings to be fitted

S_A and S_M=wetted surface area of the model with and without bossings

v_M=speed of the model

In Fig. 4 are shown ΔC_A on a base of $Rn_A=v_M(0.5\Delta S_A)^{1/2}/\nu_M$. Where, ν_M is the kinematic viscosity of the tank water. Resistance increase due to the bossings is nearly proportional to the wetted surface area of the bossing parts, and the variation of ΔC_A curves due to R_{nA} has similar trend to that of Schoenherr's friction line. The values of

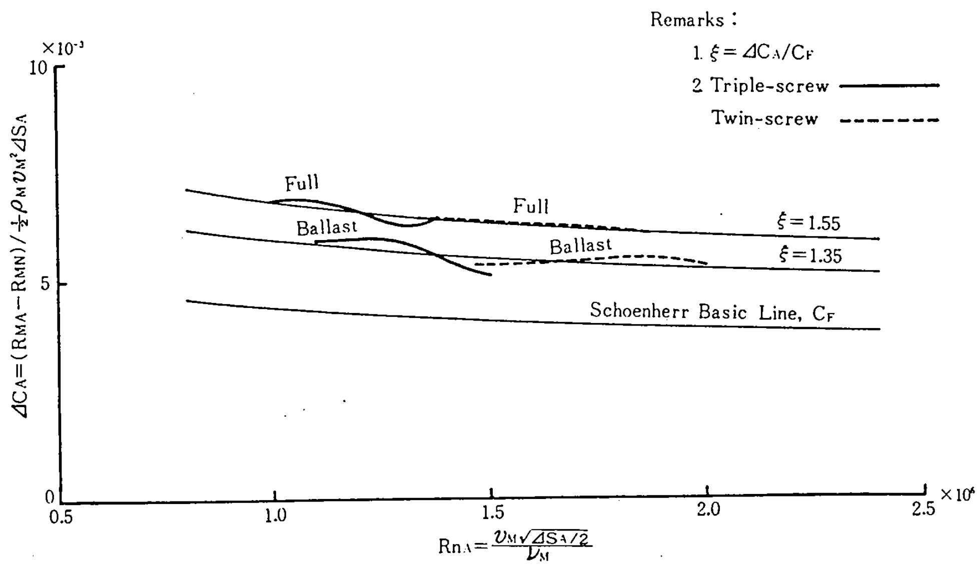

Fig. 4 Appendage Resistance

$\xi = \Delta C_A/C_F$ are given in Fig. 4 under the assumption that ΔC_A is proportional to C_F, although this relation should be studied in details before a definite conclusion can be drawn.

2.3 *Power estimation for the ships*

Power estimation for the ships were done from the model results, and the propulsive performance was compared. Total resistance R_S of the twin- and triple-screw ships was assumed to be expressed by the following formula.

$$R_S = \frac{1}{2}\rho_S S_N v_S^2 \{C_{MN} + (1+k_N)C_{FSO} + \Delta C_F\} + \frac{1}{2}\rho_S \Delta S_A v_S^2 \cdot \xi C_{FSA} \quad (2)$$

Where,

C_{MN} = wave resistance coefficient at the naked conditition

K_N = form factor of resistance at the naked condition

C_{FSO} and C_{FSA} = frictional resistance coefficient of the ship hull and appendages, respectively

The above formula implies that three dimensional extrapolation method was applied for the naked hull and ξ for the appendages. For the single screw ship is used only the first term of the right hand side of the equation (2). 0.10×10^{-3} and 0.15×10^{-3} were adopted as ΔC_F values for the fully loaded and ballast conditions, respectively, for all the ships.

Concerning the scale effect of the self-propulsion factors, only the scale effect of the wake is taken into consideration. According to the trial results of similar ships and self-propulsion test results of geosims[5], 1.10 was used as $\varepsilon = (1-w_S)/(1-w_M)$ for the center propeller of the tripple screw ship and single screw ship and 1.05 for the twin screw ship and the wing propellers of the triple screw ship. Strictly speaking, ε values must vary with aft-body shape. But, the difference will be too small to affect the results of power estimation.

EHP and SHP calculated thus are shown in Fig. 5, in a form of ratio. SHP values are lowest for the single screw ship and highest for the twin screw ship. According to the comparison in speed around the economical out-put between the twin- and triple-screw ships, the triple screw ship is superior by 0.2 knots at the fully loaded condition and by 0.4 knots at the ballast condition.

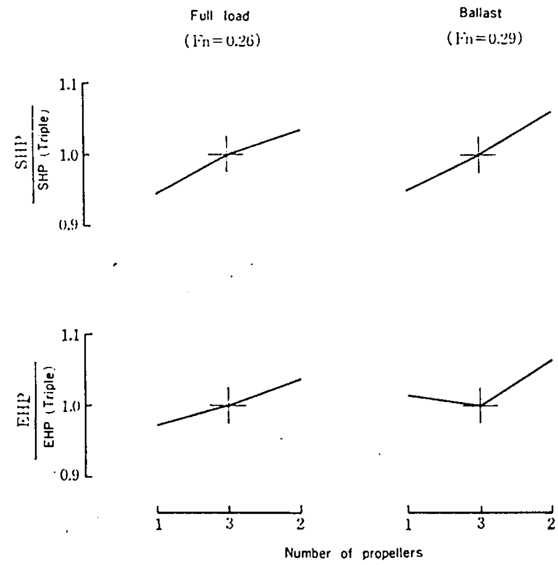

Fig. 5 Comparison of Effective and Shaft Horsepowers among Single-, Twin- and Triple-Screw Ships

3. Mutual Interference among the Ship's Hull and Propellers

3.1 *Mutual interference between the center and wing propellers*

Arrangement of the propellers and propeller shafts of the triple-screw ship is shown in Fig. 6. The shafts of the wing propellers have a inclination of 23/1000 vertically and 44/1000 horizontally. In order to know the mutual interference between propellers, the following model tests were performed.

3.1.1 *Wake measurements*

Keeping no. of revolutions of the center propeller (or the wing propellers) constant to be the same as in the ordinary self-propulsion test, the model ship was towed at the same speed as the self-propulsion test and the wake at the position of the wing propellers (or the center propeller) was meas-

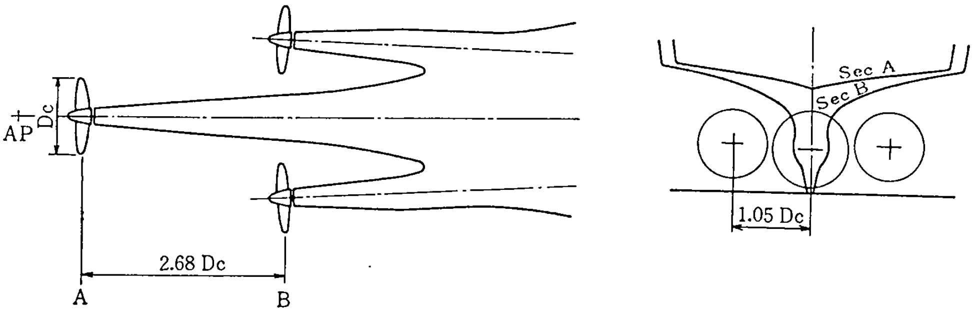

Fig. 6 Arrangement of Propellers and Propeller Shafts

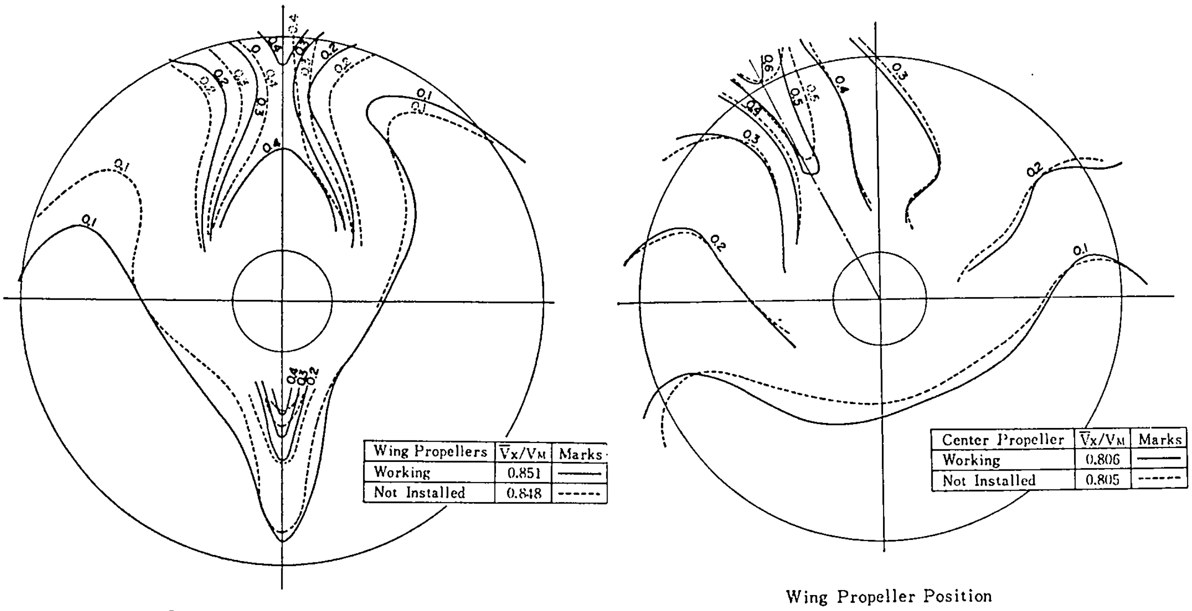

Center Propeller Position

Wing Propeller Position

Fig. 7 Wake Contours at Propeller Positions (Triple-screw, Full Load)

ured by 5-hole pitot tubes. As be shown in Fig. 7, wake patterns are nearly the same between with and without the other propellers. Difference in mean values of $(1-w_N)$ at the propeller disc between the two conditions is a little less than one percent. Also there is little difference in the tangential velocity at the propeller disc.

3.1.2 *Self-propulsion tests with only the center or the wing propellers working*

Self-propulsion tests only with the center propeller (or the wing propellers) working were carried out, adding the balancing weights corresponding to the thrust to be borne by the wing propellers (or the center propeller). The rate of the load obtained from the ordinary self-propulsion tests is

$$\left.\begin{array}{l} \beta_C = T_C/(T_C+2T_W) \\ \quad \text{for the center propeller} \\ \beta_W = 2T_W/(T_C+2T_W) \\ \quad \text{for the wing propellers} \end{array}\right\} \quad (3)$$

and therefore, the balancing weights are

$$\left.\begin{array}{l} \Delta R+\beta_W(R_M-\Delta R) \\ \quad \text{in the self-propulsion test} \\ \quad \text{only with the center} \\ \quad \text{propeller} \\ \Delta R+\beta_C(R_M-\Delta R) \\ \quad \text{in the self-propulsion test} \\ \quad \text{only with the wing} \\ \quad \text{propellers} \end{array}\right\} \quad (4)$$

where R_M is total resistance of the model obtained at the resistance test and ΔR skin friction correction at the ordinary self-pro-

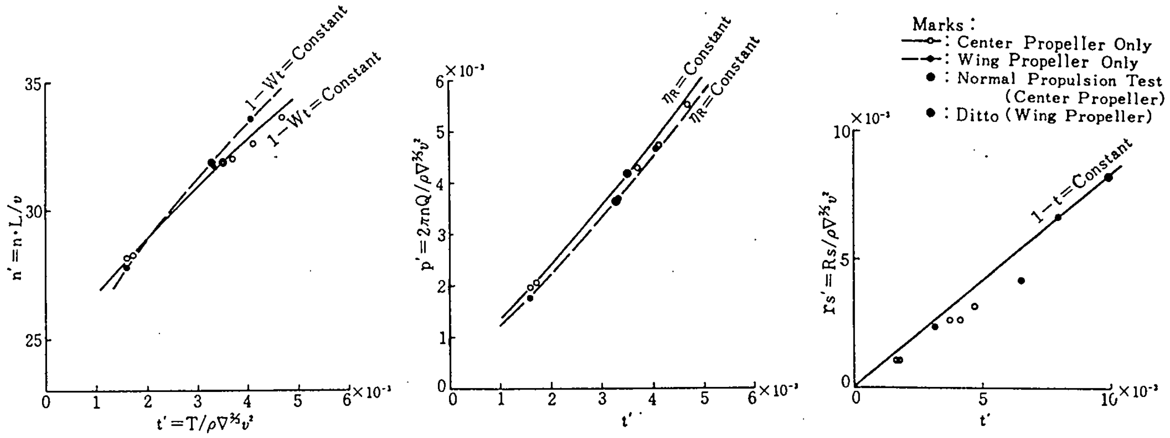

Fig. 8 Results of Propulsion Test with Only Center or Wing Propellers Working (Triple-screw, Full Load, F_N=0.27)

pulsion test.

β_C and β_W do not vary so much in the practical speed range, so that constant values were used. Moreover, to know the effect of the variation in the propeller load upon the self-propulsion factors, tests with varying β values were carried out too.

The test results are shown in Fig. 8. In the $n'\sim t'$ diagram, it is shown that $(1-w)$ obtained from these tests is coincided well with that from the ordinary self-propulsion test, which supports the results of wake measurements above mentioned. $(p'\sim t')$ diagram shows that η_R values are not different so much from those obtained by the ordinary self-propulsion test. However, $(r'_S\sim t')$ diagram gives a little different result, that is, the values of $(1-t)$ become smaller with the decrease of t'. Variation of the pressure field in the vicinity of the propeller is considered to cause the variation of $1-t$. This effect is greater in a case of the smaller thrust of the propeller and for the center propeller located at ship's center plane.

3.2 *Balance in no. of revolutions between the center and wing propellers*

3.2.1 *Effect of load condition*

If the draft and or trim were changed, no. of revolutions of the propeller at a certain out-put of the engine will vary owing to the variation of the resistance and the wake of the ship. In order to clarify the effect upon the resistance and self-propulsion factors of the trim and the displacement, the self-propulsion tests at various conditions were carried out on the triple-screw ship model. In these tests draft of the stern was kept constant, to keep the same propeller immersion.

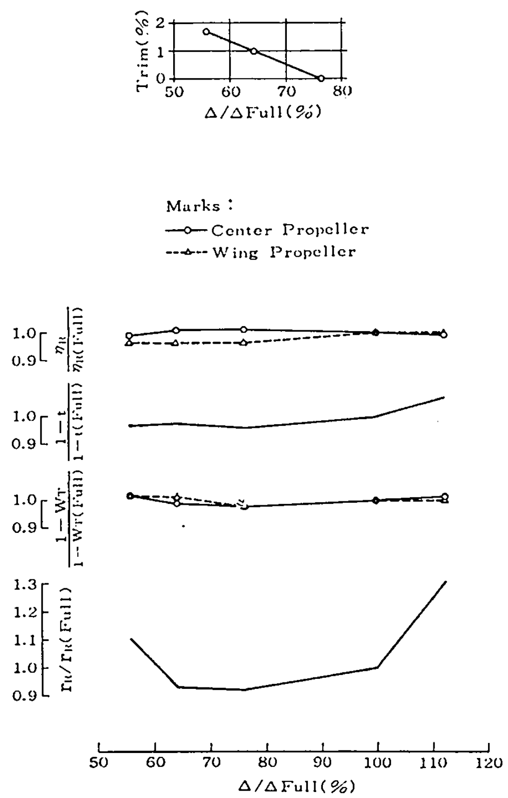

Fig. 9 Results of Resistance and Propulsion Tests at Various Loaded Conditions (Triple-screw, F_N=0.29)

The test results are shown in Fig. 9. Even on the triple-screw ship with the peculiar afterbody shape the effect upon the r_R and self-propulsion factors of the load condition is very similar to that on ordinary single screw ships.

According to the calculation using these test results, no. of revolutions of the propeller at the ballast condition are higher by about 2% for the center propeller and by about 4% for the wing propeller than that at the fully loaded condition, respectively. These amounts of difference in no. of revolutions will not cause any trouble to the revolution balance.

3.2.2 *Self-propulsion test with different no. of revolutions between the center and wing propellers*

If the out-put of the center propeller or the wing propellers were varied, the thrust of each propeller and the balancing in no. of revolutions will vary. In order to know the mutual interference between the propellers in this case, special self-propulsion tests were performed with varying no. of revolutions of the center propeller or the wing propellers on the above-mentioned model. In these tests, keeping no. of revolutions of the center propeller (or the wing propellers) constant, no. of revolutions of the wing propellers (or the center propeller) was adjusted to obtain the same ship speed as at the ordinary self-propulsion test, corresponding to the variation of the balancing weights. Denoting the skin friction correction at the ordinary self-propulsion test as ΔR,

$$R_S = R_M - \Delta R$$

Where, R_M=total resistance of the model.

Amount of variation of the balancing weight was nearly equal to 15% of R_S. The

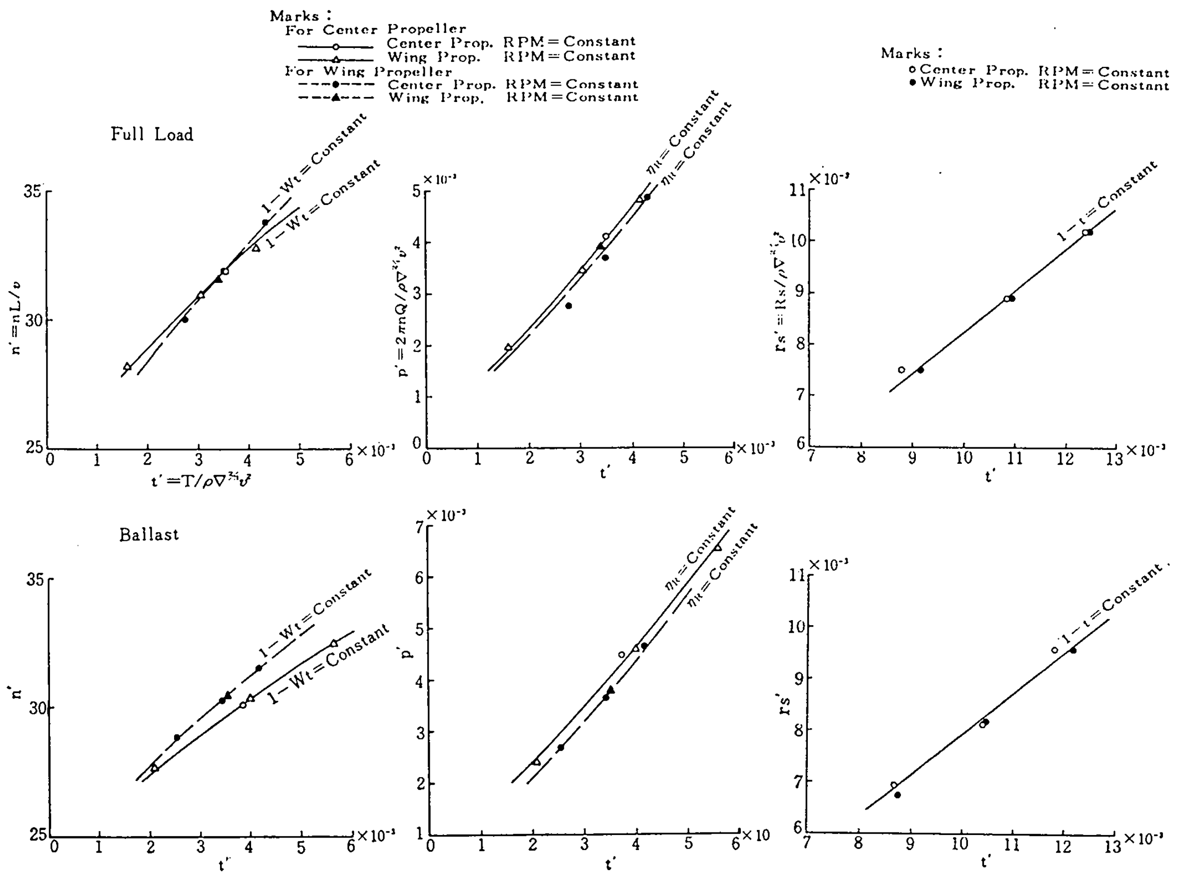

Fig. 10 Results of Propulsion Test with Center and Wing Propellers Working in Different Revolutions (Triple-screw, F_N=0.27)

test results are shown in Fig. 10, in a similar form to Fig. 8. Since it was difficult to adjust no. of revolutions of the propeller so that the model may attain the designated speed, some scatters will be seen in the plotted points. However, it may be considered that the values of self-propulsion factors do not vary with the variation of the amount of balancing weights. Therefore, estimation of the power can duly be done using the values of the self-propulsion factors obtained at the ordinary self-propulsion test, even if the state of balance were changed between the propellers.

3.3 *Effect of direction of rotation of the wing propellers*

It was reported in some papers[6] that inward rotation of the wing propellers gave the better propulsive efficiency than the outward rotation. And also, it is generally said that the outward rotation of the propellers is superior for the full hull forms and the inward rotation for the high speed vessels. These results seem to be based upon the relation between the angular velocity of the propeller and the flow near the propeller effected by the hull form and angle of attachment of the bossings.

Where the propeller shafts are covered with large and long bossings like shown in Fig. 2, outward turning flow will be generated and the tangential velocity in the propeller disc be added to the angular velocity of the propeller, which will be understood from Fig. 11. In order to know this state, the following investigations were carried out.

3.3.1 *Streamline observation around the bossings of the wing propellers*

Direction of the flow around the bossing of the wing propeller was observed on a 2 m model by the tuft grid method in the circulating tank, and existence of the flow turning outward around the bossing was recognized near the propeller.

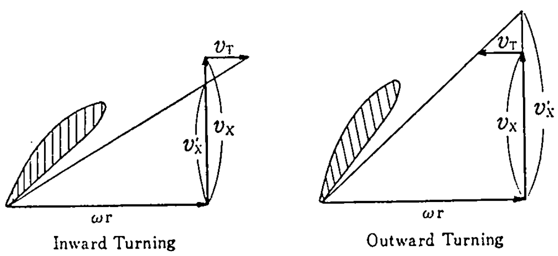

Fig. 11 Velocity Diagrams

3.3.2 *Wake measurements by-5-hole pitot tubes*

The characteristics of the tangential velocities were obtained from the results of wake measurements by-5-hole pitot tubes described in 3.1, as be shown in Fig. 12. Outward component of tangential velocity is larger at the wing propeller position than inward one, which agrees with the results of the flow observation. Taking the tangential velocity into consideration, the apparent wake fractions were obtained quasi-stationarily from the results shown in Fig. 12, which are given in Table 2. Notations used in this table are illustrated in Fig. 11. The results of this calculation agree well in tendency with the $(1-w_T)$ values obtained at the self-propulsion test which will be given in the next section, and support the discussion that inward rotation of the wing propeller are advantageous in the propulsion point of view.

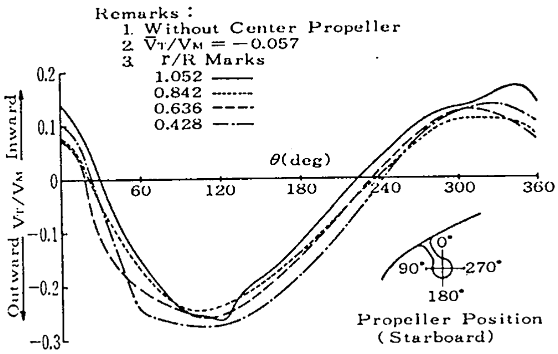

Fig. 12 Tangential Velocity at the Position of Wing Propeller

3.3.3 *The self-propulsion test with the wing propellers rotating inward and outward*

The self-propulsion tests were carried out both with the wing propellers rotating inward and outward on the triple screw ship model described in the Chapter 2. The same propellers were used for both conditions of propeller rotation. The self-propulsion factors

Table 2 Calculation of Apparent Wake Fraction (Full Load)

Direction of Turning	Outward	Inward	Remark
$\bar{v}_X/v_S$ $(=1-w_N)$	0.805		Measured by 5 hole P. Tube
$\bar{v}_T/v_S$	-0.057	0.057	
$\omega r/v_S$	1.76		Designed value
$1+\bar{v}_T/\omega r$	0.968	1.032	
$\bar{v}'_X/v_S$ $(=1-w'_N)$	0.832	0.780	$\bar{v}'_X=\bar{v}_X/(1+\bar{v}_T/\omega r)$
$(1-w'_N)/(1-w_T)$	1.03	1.03	$1-w_T$=propulsion test result

$\bar{v}_X$, $\bar{v}'_X$=Volumetric mean of v_X, v'_X (see Fig.7)
$\bar{v}_T$=Volumetric mean of v_T (see Fig. 12)

Table 3 Comparison of Self-Propulsion Factors, etc. between Inward and Outward Turning of Wing Propellers

Load condition	Full load		Ballast	
Position of propeller	Center	Wing	Center	Wing
$\eta_{R\,\mathrm{IN}}/\eta_{R\,\mathrm{OUT}}$	0.98	0.93	1.00	0.91
$(1-t)_{\mathrm{IN}}/(1-t)_{\mathrm{OUT}}$	1.04		1.04	
$(1-w_T)_{\mathrm{IN}}/(1-w_T)_{\mathrm{OUT}}$	1.01	0.87	1.01	0.87
$\mathrm{SHP}_{\mathrm{IN}}/\mathrm{SHP}_{\mathrm{OUT}}$	0.94		0.94	

in the speed range around the normal output are compared in Table 3. When the propellers rotate inward, $(1-w)$ decreases remarkably and the variations of η_R and $(1-t)$ are slight, compared with when the propellers rotate outward. Supposing a case where the same no. of revolutions were given both for outward and inward rotation of the propellers, shaft horse powers were calculated. According to this calculation, inward rotation gives about 6 percent less horsepower both at the fully loaded and ballast conditions. It is noted, however, this fact depends on the aft-body shape near the stern and the way of supporting the shafts.

4. Propeller Cavitation

4.1 *Inspection of the problem*

The propeller load per a shaft is smaller on the triple screw than on the twin screw. But, wake patterns at the center propeller have a heavy non-uniformity like a single screw ship. Moreover, the speed of advance of the propeller becomes larger and therefore, the cavitation number becomes smaller.

Consequently, the center propeller should be designed at a rather severe condition from the cavitation point of view.

The cavitation problem was investigated in details on the center propeller, and the method of improving the cavitation characteristics was applied also to the wing propeller.

When the research was begun, the following facts were known.

1) The bulbous stern intending to make the circumferential wake distribution uniform is useless and rather becomes a cause

for the resistance increase, if the frameline shapes were modified only within the limitation in designing.

2) It is difficult to improve the cavitation characteristics in such a design as the blade has most of the lift by the camber.

3) In a case of the blade sections of the propeller of the ordinary design charts, the camber is determined for a certain blade thickness. Therefore, the camber sometimes becomes too large because the blade thickness and the camber can not be chosen independently. On such a blade section, harmful cloud cavitation, liable to be a cause for errosion, often occurs at the mid-chord and the trailing edge.

If the nose of the blade section was raised up as shown in Fig. 13, increase in angle of attack of the flow to the blade will enlarge the area covered with the sheet cavitation near the leading edge but decrease in camber will avoid the cloud cavitation.[7] This sheet cavitation has nothing to do with the errosion, and this amount of correction at the leading edge scarcely varies the lift.[8]

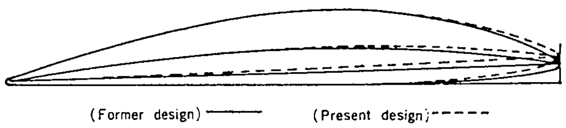

Fig. 13 Modification of Blade Profile

Taking the fact above mentioned into consideration, screw propellers were designed and their cavitation characteristics were improved through the cavitation tests. That is, lift distribution was obtained by the method to design wake-adopted propellers, which is adopted at NSMB.[9] Then, blade thickness breadth ratio was determined from the cavitation diagram[10] on the propellers with the AU type section, and pitch ratio by Nakajima's formula.[11] As the blade section were designed four types of blades, based upon the blade sections of AU type.

First of all, blade A was designed by cutting up the leading edge of AU type of blade section at an aim to prevent the cloud cavitation by increasing the angle of attack and decreasing the camber. Then, Blade B and C were designed by sharpening the leading edge, expecting to suppress the cloud cavitation taking place at the leading edge by making the pressure drop larger and then the area covered with the sheet cavitation wider. The blade thickness was slightly decreased along 10% of chord length for Blade B and along 25% for Blade C at the back side near the leading edge. Blade D was designed by decreasing the blade thickness at the back side of the blade section around the mid-chord, the object of which is to increase the effect to prevent the cloud cavitation by making the chamber smaller. Profiles of Blades A, C and D are shown in Fig. 14.

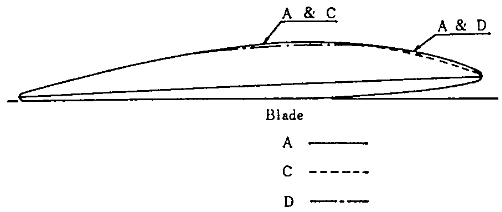

Fig. 14 Profiles of Blade A, C and D

4.2 *Cavitation test*

A six-bladed propeller was manufactured with the four kinds of blades above mentioned, and the cavitation test was performed in the non-uniform flow. In Fig. 15 is shown the wake distribution reproduced by

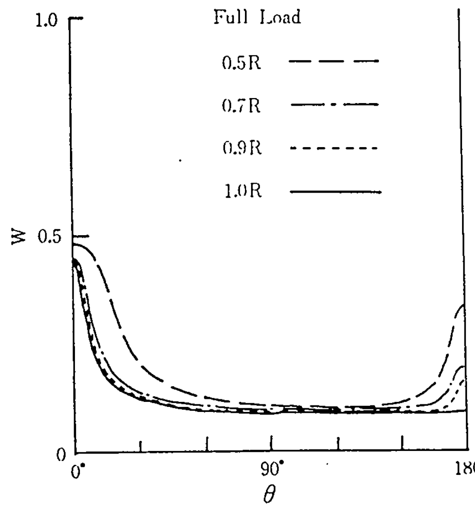

Fig. 15 Wake Distribution (Full Load)

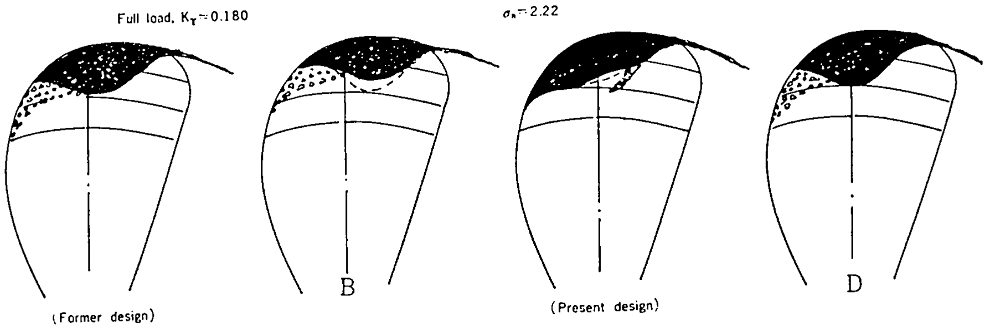

θ=9° starboard from the top of screw aperture

Fig. 16 Comparison of Cavitation Patterns

the wire-mesh in the cavitation tunnel, which is similar to the longitudinal wake distribution measured by 5-hole pitot tubes at the center propeller position with the wing propellers rotating inward at the fully loaded condition. As an example for the test results, comparison of the cavitation patterns among the four blades at $\theta=9°$ is shown in Fig. 16.

There were no cavitation on the face side of all the blades, but on the back the followings were noticed.

1) At the leading edge of 0.7~0.9 R on the Blade A took place small pieces of cavitation, looking like the bubble at a glance. This kind of cavitation has not been experienced and was found to be of thin film by the detailed observation. It is understood that owing to small pressure drop at the leading edge the cavitation occurred in this part could not grow into the sheet cavitation and came out as pieces of cavitation of thin film. In the neighbourhood of $\theta=18°$ appears the cloud cavitation at 0.8~0.9 R of the trailing edge, which is considered to have been transformed from the sheet cavitation caused by the peak of the negative pressure near the mid-chord due to too large camber in the vicinity of 0.8~0.9 R.

2) The state of cavitation on the Blade B is quite similar to that on the Blade A. Stationary sheet cavitation took place on the Blade C. This cavitation is considered to be caused by the large pressure drop due to the sharp profile at the leading edge.

3) Expected effect did not appear on the Blade D, which seems to be based on the too small change in camber.

According to the results above mentioned, two corrections of cutting up the blade section as shown on the Blade A and sharpening the leading edge as shown on the Blade C were adopted for the blade section of the full scale propellers.

5. Full Scale Measurements and Correlation with Model Results

5.1 *Speed trial*

Progressive speed trials with two or three screws working were carried out at the sea trial of the triple screw ship, and some data with only the center propeller working were taken during her navigation before the trial. All the tests were performed at 65% displacement of the full load's and 1% trim by the stern of L_{pp} which corresponds to the ballast condition of the model.

5.1.1 *Progressive speed trial*

In this test, the engine load was varied progressively by four steps, keeping no. of revolutions of the center and wing propellers to be those at the normal operation of the engine, and speed of the ship, shaft horse power and no. of revolutions of the propellers were measured at each run of four groups.

The sea state was not so good with wave scale 3 and Beaufort scale 5~6, and because the wind direction was coincided with the direction of ship's runs, difference in speed between both runs of going and returning attained to more than one knot. Correction for the wind was made by Taniguchi and Tamura's method,[12] and results of measurements were corrected to the standard condition of no wind nor current. This result was coincided well with the power curve estimated from the model tests described in Chapter 1. In order to know the correlation between ship and model, analyses of wake scale effect ε and roughness allowance ΔC_F were carried out on the results converted to the standard condition. These analyses were made by the usual method[13] and scale effect on propellers was not taken into consideration. ε was 1.07 for the center propeller and 1.09 for the wing propellers, which are a little different from the values estimated in Chapter 1. ΔC_F values were very near to 0.15×10^{-3} estimated by the three dimensional extrapolation method of equation (2), in which the appendage resistance was treated separately. In order to know which extrapolating method will be suitable, following two methods were compared with the method of equation (2). The first one is expressed by

$$R_S=\frac{1}{2}\rho_S S_N v_S^2\{C_{WN}+(1+K_N)C_{FSO}+\Delta C_F\}+\frac{1}{2}\rho_S\cdot\Delta S_A\cdot v_S^2\cdot\frac{1}{2}\Delta C_A \qquad (5)$$

In this method 1/2 of appendage resistance coefficient ΔC_A, is added to the hull resistance. This method[14] has been used rather often. The other one is a method in which the appendage resistance is not separated from the hull resistance, and expressed by

$$R_S=\frac{1}{2}\rho_S S_A v_S^2\{C_{WN}+(1+K_A)C_{FSO}+\Delta C_F\} \qquad (6)$$

Where, suffix N implies the naked condition and A with appendages.

Assuming ΔC_F values as 0.15×10^{-3}, effective horse power was calculated by three equations of (2), (5) and (6) and their results were compared with the results obtained at the trial of the ship in Fig. 17. As be seen from this figure, equations (2) and (5) give good agreements with the trial results, but equation (6) gives too large estimation for EHP. So, equation of (2) or (5) seems to give better results.

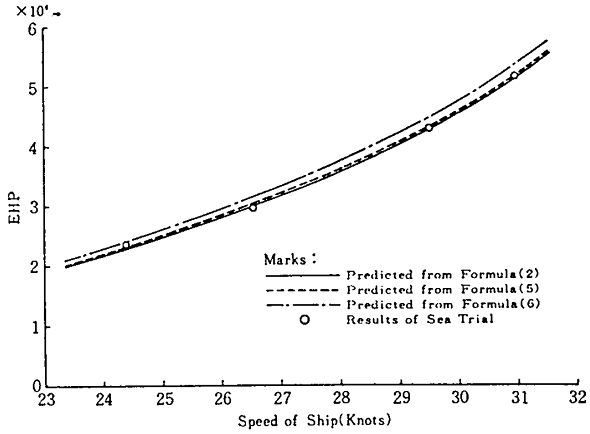

Fig. 17 Comparison of EHP Curves between Predicted and Sea Trial Results

5.1.2 *The speed trial with center or wing propellers loosing*

The ship speed, shaft horse power and no. of revolutions of the propellers were measured in a group of runs at the engine load to absorb the maximum torque of the engine with only the wing propellers (or the center propeller) working and with the center propeller (or the wing propellers) loosing. This test gives an interesting data as an example of quite different state of balance in no. of revolutions, but as only one group of runs was performed detailed discussion can not be made. Therefore, paying attention only to the relation between the propeller load and wake fraction, $(1-w_Q)$ values obtained from this test on torque identity method are compared with the results of the progressive speed trial, which is shown in Fig. 18. In this figure are also shown the results of the model tests to give some idea of ship model correlation. The 'Center propeller only' in this figure means the data obtained when the ship was run with only the center propeller and without the wing propellers before the speed trial. In this case, the ship speed was read from the indicator of an electromagnetic log and measurement of shaft horse power may not always be done so accurately

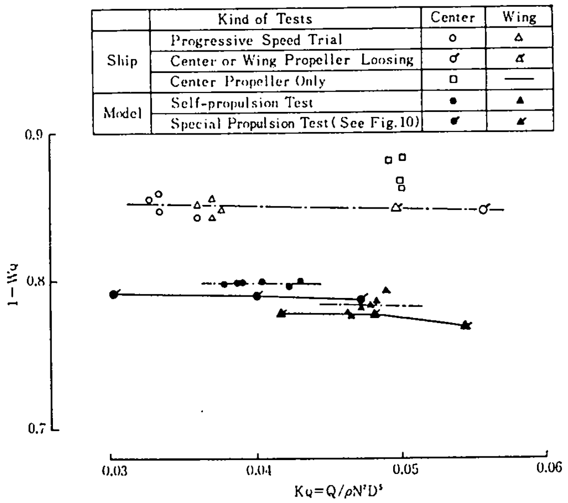

Fig. 18 $1-w_Q$ Versus K_Q at Various Kinds of Propulsion Tests on Both Model and Ship

as at the speed trial. However, this kind of data can seldom be obtained on a full-scale ship, so it was shown without hesitation.

$(1-w_Q)$ values are not varied so much with the torque coefficient K_Q, which were obtained from the measured shaft horse power and no. of revolutions of the propellers. K_Q values are considered to show a scale of the propeller load, so it is deduced that even this amount of considerably large variation in the propeller load is not so influencial on the wake fraction. The results of the model tests also give a similar tendency in this point.

5.2 *Observation of the propeller cavitation*

Full-scale observations of the propeller cavitation were carried out at the sea trial, only on the center propeller. In order to make the observations easier through the observation window at a sufficient depth under the water surface, the draft of the stern was taken larger than at the speed trial, which resulted in satisfactory observation up to the high speed.

Observations were made at four load conditions of the engine, and in one condition of them the wing propellers were made near to be loosen and the load of the center propeller was made considerably heavier. Arrangement of the observation windows and instruments are similar to those described in the literature (15).

An example for the cavitation patterns observed is shown in Fig. 19. Angular positions of the propeller observed are within a range of 30∼50° starboard side from the top. The cavitation patterns are not so different in this range of angular positions. There occurred the sheet cavitation in 10∼20% of the chord length at the leading edge of 0.7R∼the tip, and the cloud cavitation took place near the mid-chord of 0.975R and

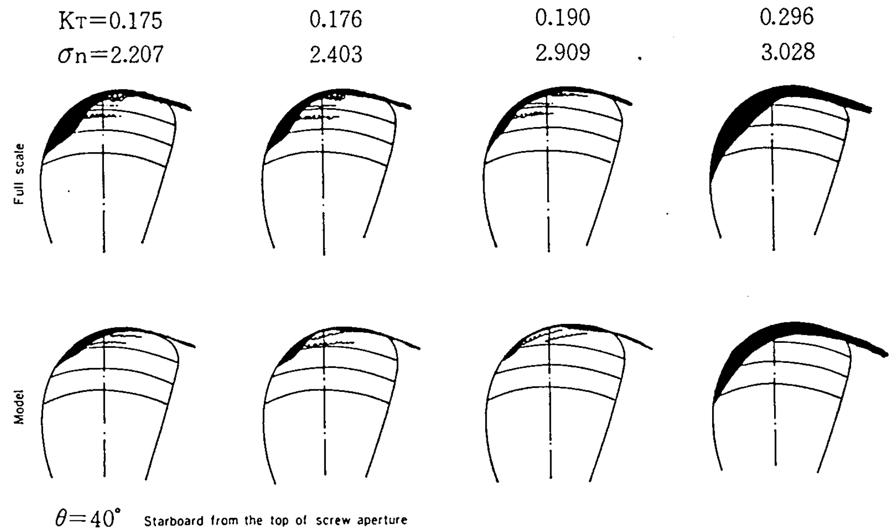

Fig. 19 Comparison of Cavitation Patterns of Center Propeller between Full Scale and Model

from the rear edge of the sheet cavitation of 0.85 R~0.9 R. The extent of cavitation occurrence is narrow and the cloud cavitation is weak, which is considered to be based upon the effect of decreasing the propeller load by distributing the horse power in three shafts and of adoption of an aerofoil section with large cutting up at the leading part and a little thinner blade thickness of the leading part.

In order to inspect the correlation between ship and model, the cavitation test was performed in non-uniform flow on the model propeller corresponding to the full-scale, the scale ratio being 1/32.5 (dia.=200 mm). The wake distributions reproduced in the cavitation tunnel are shown in Fig. 20. The cavitation number σ_n used in the test is obtained

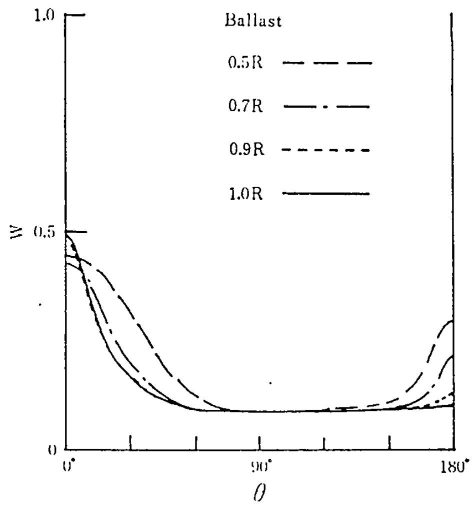

Fig. 20 Wake Distribution (Ballast)

from the static pressure at the shaft center line and no. of revolutions of the propeller during the full-scale observation. The thrust coefficient K_T was obtained from the torque coefficient measured at the full-scale observation and open test results of the model propeller.

An example for the test results of the model propeller is shown in Fig. 19. Summary of the results is as follows:

1) In a case of small K_T, the sheet cavitation occurs by 3 to 5% of the chord length at the leading edge of 0.85 R~the tip on the back side of the blades. The cavitation pattern is different from that of the ship and the extent of cavitation is smaller. The cloud cavitation takes place near 0.9~0.95 R on the back side, but the position of the cavitation is different from that of the ship and its strength is weaker.

2) In a case of K_T=0.296, the cavitation pattern and extent of the cavitation on the model propeller are quite similar to those on the actual propeller.

3) In both cases, no cavitation can be seen on the face of the propeller.

The difference in cavitation between ship and model described in 1) is similar to the results obtained by the three full-scale measurements[16] on propeller cavitation already done, and its reason has already been proved.

Concerning the difference between 1) and 2) above mentioned the followings may be considered. Although the angle of attack of the flow to the blade element varies between ship and model due to the scale effect of the wake distribution, this difference does not vary with the variation of the propeller load. In a case of light load, that is, when the angle of attack is small, the variation of the angle of attack influence sensitively on the occurence of the cavitation. In a case of heavy load, however, and when the cavitation has grown sufficiently, the cavitation pattern does not vary with the variation of the angle of attack.

6. Concluding Remarks

In constructing a triple screw container ship, many basic investigations and various kinds of model tests were carried out, and expected results were obtained by introducing the test results into the design of the hull form and propellers.

Principal conclusions obtained are as follows:

1) On such a high speed container ship as investigated here, triple screw propulsion gives the better propulsive performance than twin screw propulsion.

2) The triple screw ship adopted showed

better propulsive performance with the wing propellers rotating inward, the reason of which is explained by the wake measurements using 5-hole pitot tubes and by the results of the self-propulsion tests.

3) Mutual interference between the propellers can not be seen for the propeller arrangement of this triple screw ship.

4) The effect of variation of the propeller load upon the propeller performance is negligible for each propeller except upon the propeller efficiency, unless the variation of the propeller load is large.

5) In order to avoid the back cavitation of the center propeller, it is effective to change the shape near the leading edge so as to decrease the camber and increase the angle of attack, which is also supported by the full scale observation.

6) The results of the speed trial of the ship were coincided well with those estimated from the model results. It gives a key to the scale effect problem. It may be better to consider that the appendage resistance is also subject to the scale effect.

Finally, the authors express heartily thanks to the people concerned in this research project, especially to Osaka Shosen Mitsui Senpaku Co., Ltd. and Tamano Works, Mitsui Shipbuilding and Engineering Co., Ltd. for their cooperation in performing the full scales measurements.

References

1) Council Transport Technics: Report of 1st Meeting of the Committee of Ships, No. 8, 1970
2) K. TSUCHIDA and T. WATANABE: Tank Experiments of Triple-Screw Small Tanker, Report of the Transportation Technical Research Institute, Vol. 3, No. 3, 1953
3) Y. SUGIMURA and M. ABE: Model Experiments on the Effect of Block Coefficient with High Speed Cargo Vessel, Mitsui Technical Review, No. 63, 1968
4) A. YAZAKI and Others: Extension of the Design Charts of AU-Type Four and AU_w-Type Six Bladed Propeller Series to High Pitch Ratio, Journal of the Society of Naval Architects of Japan, Vol. 131, June, 1972
5) K. YOKOO and Others: Scale Effect Experiments on Models for High Speed Cargo Liners, Abstract Note of the 16th General Meeting of Ship Research Institute, 1970
K. YOKOO and Others: Scale Effect of Full Hull Form with Various Stern Shapes, Journal of the Society of Naval Architects of Japan, Vol. 128, Dec. 1970
6) K. YOKOO and Others: Investigation into the Propulsive Performance of High Speed Container Ships (1st Report) —Effects of Stern Shape and Appendages for the Twin-Screw Ships—, Abstract Note of the 18th General Meeting of Ship Research Institute, 1971
J. FATUR: Maierform Comments of Modified Hull Form, Shipbuilding and Shipping Record, Sept. 1969
E. ENKVIST: The Cable Ship "Ingul", The Shipbuilding and Marine Engine-Builder, Jan. 1963
7) H. KADOI: Propeller Cavitation (2)—Effect of Decreasing the Blade Camber to Avoid Harmful Cavitation, Bulletin of the Society of Naval Architects of Japan, No. 519, Sept. 1972
J.D. VAN MANEN: Bent Trailing Edges of Propeller Blades of High Powered Single Screw Ship, Proc. of IAHR Symposium of Cavitation and Hydraulic Machinery, Sendai, Japan, 1962
8) K. SUGAI: The Propeller Lifting Surface Theory and Its Applications, Proceedings of the 2nd Symposium of Marine Propeller, the Society of Naval Architects of Japan, Nov. 1971
9) J. D. VAN MANEN: Fundamentals of Ship Resistance and Propulsion, Part B Propulsion, I.S.P., Vol. 4, Nos. 30-37, 1957
10) T. ITO, H. KADOI and Others: Measurements of Pressure Distribution on Sections for the MAU Propeller, Abstract Note of the 14th General Meeting of Ship Research Institute, 1969
11) Y. NAKAJIMA: A New Criterion of Cavitation for Screw Propeller, Journal of the Society of Naval Architects of Japan, Vol. 92, 1957
12) K. TANIGUCHI and K. TAMURA: On the New Method of Correction for Wind Resistance Relating to the Analysis of Speed Trial Results, Journal of the Society of Naval Architects of West Japan, Vol. 18, Aug. 1959
13) J.T.T.C.: Draft of Standard Trial Analysis Code for Large Ships, Bulletin of the Society of Naval Architects of Japan, No. 442, 1966
14) J.T.T.C.: Text of the 1st Towing Tank Symposium, the Society of Naval Architects of Japan, 1959

K. TANIGUCHI: Model-Ship Correlation Methods in the Mitsubishi Experimental Tank, Journal of the Society of Naval Architects of Japan, Vol. 113, 1963

15) T. ITO, H. KADOI and Others: Full Scale and Model Observation on Propeller Cavitation, Journal of the Kansai Society of Naval Architects of Japan, Vol. 135, 1970

16) T. ITO and H. KADOI: Cavitation of Marine Propeller (2), Proceedings of 2nd Symposium on Marine Propeller, the Society of Naval Architects of Japan, Nov. 1971